Self-Powered Active Spherical Triboelectric Sensor for Fluid Velocity Detection

Ping Cheng, Mingchao Sun, Chunlei Zhang, Hengyu Guo, Jihong Shi, Yi Zhang, Yina Liu, Jie Wang, Zhen Wen, and Xuhui Sun, *Senior Member, IEEE*

***Abstract*— Developing fluid velocity sensors with high accuracy, high stability and self-power has practical significance. Triboelectric sensors provide a strategy to realize high-performance self-powered active sensing. In this article, we present a fully enclosed self-powered active spherical triboelectric sensor (SASTS) to detect the fluid velocity. Based on the electrification at the contact interface, resulting in the electrostatic induced electrons transferring between two interdigitated electrodes, SASTS effectively harvests the fluid flow energy to electric signal. After Fourier transform processing of the output signal, the motion frequency of the SASTS can be distinguished and the fluid velocity can be further calculated. By optimizing the structure parameter, it features high precision with average standard deviation less than 4, wide range speed from 2 m/s to 18 m/s of fluid flow, and proved lifetime more than half a year. This technique can be applied to measurement of fluid flow speed, even potentially to other rotation movements, which could have wide applications, such as environment monitoring, transportation and so on.**

***Index Terms*—Triboelectric sensor, fluid energy, velocity detection, spherical, self-powered.**

Manuscript received November 22, 2019; revised February 3, 2020; accepted February 18, 2020. Date of publication March 2, 2020; date of current version March 13, 2020. This work was supported in part by the National Natural Science Foundation of China under Grant 61804103, in part by the Natural Science Foundation of the Jiangsu Higher Education Institutions of China (18KJA535001), in part by the Natural Science Foundation of Jiangsu Province of China (BK20170343), in part by the State Key Laboratory of Silicon Materials, Zhejiang University (SKL2018-03), in part by the Jiangsu Key Laboratory for Carbon-Based Functional Materials and Devices, Soochow University (KJS1803), in part by the XJTLU Key Programme Special Fund (KSF-A-18), in part by the Collaborative Innovation Center of Suzhou Nano Science & Technology, in part by the Priority Academic Program Development of Jiangsu Higher Education Institutions (PAPD), in part by the 111 Project, and in part by Joint International Research Laboratory of Carbon-Based Functional Materials and Devices. The review of this article was arranged by Associate Editor Dr. H. X. Zhang. *(Corresponding Authors: Mingchao Sun; Zhen Wen; Xuhui Sun.)*

Ping Cheng, Jihong Shi, Yi Zhang, Zhen Wen, and Xuhui Sun are with the Jiangsu Key Laboratory for Carbon-Based Functional Materials and Devices, Institute of Functional Nano and Soft Materials (FUNSOM), Soochow University, Suzhou 215123, China (e-mail: 20184014011@stu.suda.edu.cn; 20174014048@stu.suda.edu.cn; 20184214107@stu.suda.edu.cn; wenzhen 2011@suda.edu.cn; xhsun@suda.edu.cn).

Mingchao Sun is with the Fine Mechanics and Physics, Chinese Academy of Sciences, Changchun Institute of Optics, Changchun 130033, China (e-mail: quanquanllzz@163.com).

Chunlei Zhang and Jie Wang are with the Chinese Academy of Sciences, Beijing Institute of Nanoenergy and Nanosystems, Beijing 100083, China (e-mail: zhangchunlei@binn.cas.cn; wangjie@binn.cas.cn).

Hengyu Guo is with the Department of Physics, Chongqing University, Chongqing 401331, China (e-mail: cquphysicsghy@gmail.com).

Yina Liu is with the Department of Mathematical Sciences, Xi'an Jiaotong-Liverpool University, Suzhou 215123, China (e-mail: yina.liu@xjtlu.edu.cn).

This article has supplementary downloadable material available at http://ieeexplore.ieee.org, provided by the authors.

Digital Object Identifier 10.1109/TNANO.2020.2976154

I. Introduction

With the advanced development science, internet technology and increasing demand of people, a novel, credible and sustainable operation of sensor networks are urgently required. [1]–[3] By combining various sensors with automated systems, the information can be gathered and help us with particular tasks. Water disasters happen frequently on earth, developing a real-time monitoring system is important for fluid flow monitoring. [4], [5] Determining the real-time velocity of the fluid flow by electronic strategies rather than direct detection is a fundamental demand, especially in harsh environments. Current technologies for velocity measurements are mainly based on capacitance, [6] optical sensing, [7] electromagnetic interaction [8] and so on. These strategies, however, require a constant power source outside and sufficient space to be equipped inside the device or in the system. Self-powered active sensing refers to that the sensor itself can obtain the energy, such as light, heat or mechanical energy, and converts it to electricity signal as a response to the stimulation from the ambient environment. No any external power source is required to apply onto such a device or system. [9]–[13] Thus, it appears quite desirable to develop such a kind of self-powered active sensors for fluid velocity detection with high accuracy, high stability and long lifetime. [14]–[17]

Triboelectric sensor nowadays has been received increasingly extensive attention due to several advantages with simple mechanical structure, large design flexibility, various choices of materials, and low cost, *etc*. [18]–[21]. Coupling with triboelectrification and electrostatic induction, [22], [23] these sensors can directly convert irregular, small-scale mechanical energy into electric signal without external power, which is suitable to achieve a large-scale real-time sensor network. [24]–[27] However, there are still some critical issues to be addressed. Firstly, it is significant to fabricate a high accuracy and wide range sensor when detect the state of motion. [28] Secondly, based on the sliding mode, the friction will lead to mechanical wear of the dielectric materials, which is a huge challenge to the stability of sensor. [29]–[31] In addition, waterproof device is necessary to keep high triboelectrification effect in the outdoor environment, especially in the fluid condition. [32]–[35] Thus, how to design a self-powered active triboelectric sensor for fluid velocity detection still pose considerable challenges.

In this work, we proposed a fully enclosed waterproof self-powered active spherical triboelectric sensor (SASTS). It works by contacting electrification at the rolling interface to effectively

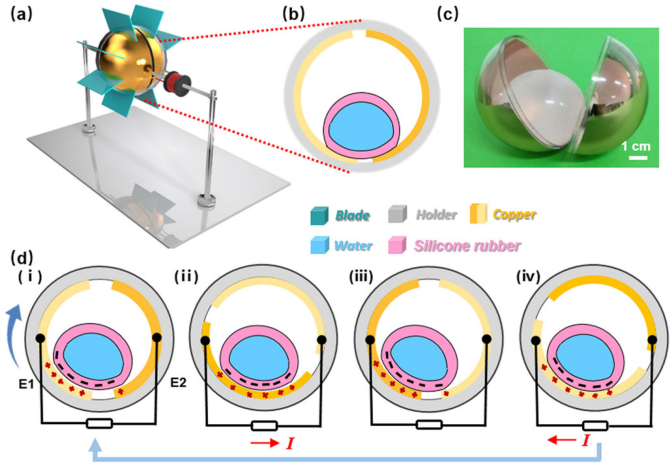

Fig. 1. Schematic illustration of the self-powered active spherical triboelectric sensor (SASTS). (a) Structural scheme of the SASTS and (b) the cross-sectional image of the triboelectric part. (c) Photograph of the triboelectric part (scale bar, 1 cm). (d) Charge distributions of the triboelectric part under a short circuit.

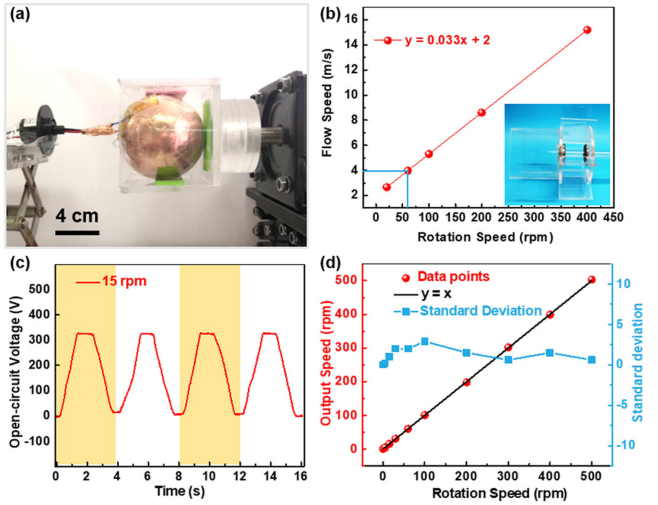

Fig. 2. Photograph and data processing of the SASTS. (a) Structural scheme of the SASTS test setup. (b) Relationship of the rotation speed of the frame and the fluid flow speed (Inset shows the image of a specific frame) (c) Output voltage signal of sensor at 15 rpm. (d) Output speed of SASTS and the standard deviation.

transform ambient vibration energy to the electric signal. By optimizing the structure parameter, the SASTS features high precision, longevity, and wide range, which is suitable to measure the rotation speed and the fluid flow speed. Based on the rolling free-standing mode, it overcomes the mechanical wear of materials. Furthermore, this SASTS is relatively easy to fabricate, and it enables to generate signals that can highly repeated.

II. Experimental Results

Fig. 1(a) is the schematic illustration of the self-powered active triboelectric spherical sensor (SASTS). It consists of a spherical part with a flexible rolling sphere, outside frame, and an electric brush, which works by driving the blades of frame and getting output signal. Fig. 1(b) illustrates enlarged cross-sectional image details of the triboelectric unit. It is composed of a 7 cm diameter outside shell with two electrodes attached and a flexible rolling sphere with some water inside to increase the gravity and keep a good movement. Fig. 1(c) is photograph of the fabricated triboelectric unit. The flexible rolling sphere is made of silicone rubber which could provide much better output performance than that of the convention solid sphere. The water was injected by the syringe to increase the inertia of the silicone rubber ball to achieve a better state of motion. When the blades are driven by fluid, the rolling ball in the inner shell will roll back and forth between two electrodes. After analyzing the data by the algorithm, the real speed of the fluid can be obtained. As illustrated in Fig. 1(d), the working principle of this sensor is the triboelectrification effect. [36], [37] Firstly, the triboelectric sphere and electrodes are not uncharged, when the dielectric material and electrode physically contact, static charges will then generated by the triboelectrification effect. When the soft sphere moves between the two separated electrodes, some negative charges will be generated on the soft sphere surface and some positive charges will be generated on the surface of copper electrode because of the triboelectric effect (state i). When the device starts rotating driven by the fluid, the inner sphere moves to the other electrode, positive charges will flow from the Electrode 1(E1) to the Electrode 2(E2) (state ii). As the outer shell continues to rotate, the inner silicone ball contacts electrode 1 again, and an opposite direction movement of the soft silicone ball from Electrode 2 to Electrode 1 will drive the positive charges moving in the same direction. (state iii). Then, the inner ball will return to the initial position (state iv) and start the next cycle. [26], [27]

The photograph of experimental setup of the self-powered active triboelectric spherical sensor is shown in Fig. 2(a). Driven by the rotary motor, it outputs the electric signal through the electric brush to avoid wire winding. Fig. 2(b) shows the relationship between a specific frame rotation speed and fluid flow speed. Each different frame has a specific linear relationship $y = ax + b$. Here, we used a frame 1 with a relationship of $y = 0.03x + 2$. The inset image is a specific frame. By changing the parameter (weight or shape) of the frame, there will be different relationships to fit various flow velocity. When the SASTS works, the silicone rubber sphere rolls between the two electrodes, alternately, the output signal can be detected by the electrometer, as shown in Fig. 2(c) and Fig. S1. At a speed of 15 rpm, the period of motion is about 4 s. Through the Fourier transform of this signal, the motion frequency of the device can be obtained and the actual speed of the sensor can be calculated. Because of the linear relationship between the rotation speed and the flow velocity, the flow velocity can also be immediately calculated. Fig. 2(d) shows the relationship of the setting rotation speed and the output rotation speed from the experimental data. A series of data points display on the perfect curve of $y = x$ (0.5 rpm to 500 rpm), which means that the output data fit well with the theoretical values. Also, the average standard deviation

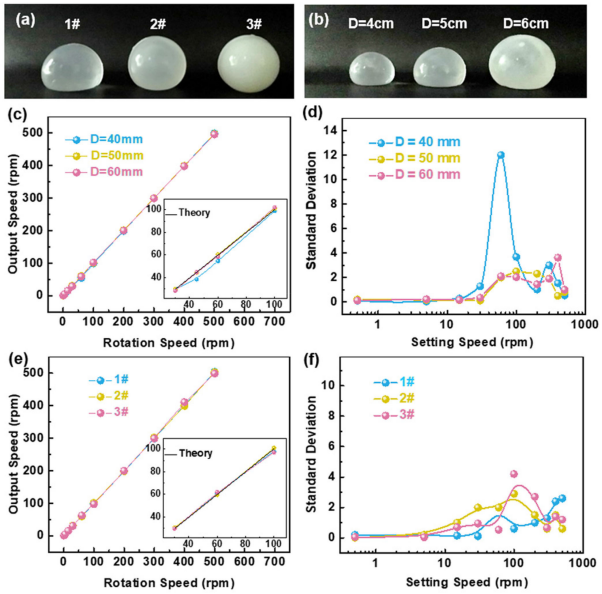

Fig. 3. Signal analysis of the SASTS. Photograph of the inner silicone rubber sphere with (a) different thicknesses and (b) different sizes. Output speed of SASTS with (c) different sizes inner balls (d) and the standard deviation. Output speed of SASTS with (e) different thicknesses inner balls and (f) the standard deviation.

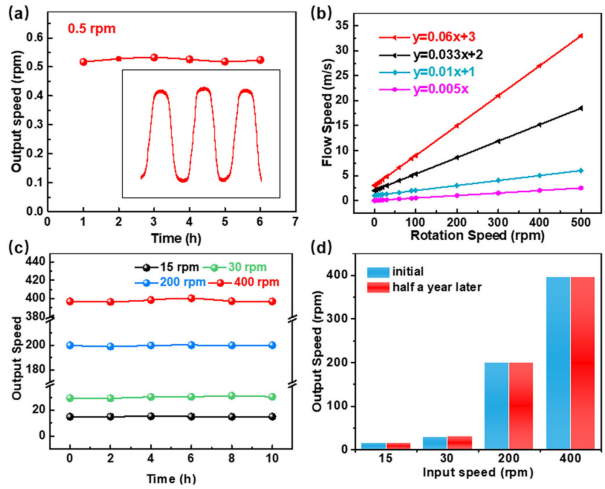

Fig. 4. Durability of the SASTS at particular conditions. (a) Output speed of the SASTS at particular condition 0.5 rpm. (The inset is the output electric signal) (b) Relationship of the flow speed and the rotation speed using different frames. (c) Long-term stability test of a SASTS (2#) in various speeds and (d) comparison of system output after 30 days of rest.

of the output is calculated to be merely less than 4. In view of the inherent error of the electronic machine (about $\pm$ 0.2%), this sensor system has a great accuracy.

To investigate the effect of softness the silicone rubber sphere on output accuracy, some spheres with different softness degree (1# = 0.28 mm, 2# = 0.42 mm, 3# = solid one) and size (D = 4 cm, 5 cm, 6 cm) of silicone are fabricated (Fig. 3(a), 3(b) and Fig. S2). The different thicknesses of the flexible ball are fabricated by controlling the volume of the silicone rubber, and different sizes of the flexible ball are molded by using diverse size shell (Supplementary Note 1). A rotary motor was used to simulate the flowing fluid. The output performance of SASTS with different sizes inner silicone rubber balls is shown in Fig. 3(c). From 0.5 rpm to 500 rpm, the size of the inner sphere does not affect the output accuracy much more. However, in the enlarged diagram, the smaller inner sphere shows a little deviation compared with the larger ones. Furthermore, the standard deviation of the SASTS with 4 cm diameter silicone rubber (SASTS D4) is much bigger than the others (Fig. 3(d)). Because the smaller inner sphere is much lighter, which is much easier to be affected at a higher speed of the outer shell. Therefore, the deviation of SASTS D4 increase over a period of time. When the speed of outer shell continues to increase, the movement state of the soft sphere will keep relatively stable. In Fig. 3(e) and 3(f), the output performance of different thicknesses flexible sphere are tested. The output values of SASTS with 1# silicone rubber ball (SASTS 1#), SASTS 2# and SASTS 3# are all fitted well. From the enlarged image, the thickness of the silicone rubber sphere almost does not affect the accuracy. Moreover, in Fig. 3(f), the standard deviation of each sensor with various thickness keeps in a small and stable value. Therefore, the accuracy of the sensor is positively related to the size of the silicone ball, but not to the thickness.

In Fig. 4(a) and Fig. S3, the SASTS presents the stable performance with wide range of output speed. At a very lower rotation speed 0.5 rpm, this device shows stable output and the electric signal is enlarged in this figure. When the rotation speed is 500 rpm, the electric signal in the Fig. S3 also maintains a steady trend. As shown in Fig. 4(b), by changing the parameter of the frame, the relationship of the flow speed and the rotation speed can be tuned to match various ambient environments. For example, the relationship y = 0.033x + 2 by using one frame can be obtained. If the rotating speed exceeds 500 rpm, there will be no output signal due to inertia. When the parameter (like mass and volume) of the frame was changed, the other relationship like y = 0.06x+3 can be fit, which is more suitable to monitor the high speed fluid. If the relationship is y = 0.01x+1 and y = 0.005x, these frames are more suitable to monitor the lower speed fluid. In addition, the stability of sensor is another significant value, 10 hours test cycles were carried out by using a rotary motor (Fig. 4(c)). The output speed of the sensor at different speeds remain almost steady. After this device sets aside for half a year, the stability of this sensor is still maintained (Fig. 4(d)).

A SASTS sensor system was built to demonstrate the detection of the fluid flow speed. The SASTS was installed on the rotary motor. When the rotation speeds are setting at different values, the experimental value would be displayed on the screen by the analysis of the software, as shown in the Fig. 5(a)–(b) and Movie S1-S2. Two setting speeds (5 rpm and 400 rpm) of the motor were tested by the SASTS, and the experimental values were 5.08, and 399.65, respectively. These values are very close to the theoretical value, which shows a pretty accuracy of the SASTS. Fig. 5(c) is the circuit diagram of the SASTS, a TENG and a voltmeter are connected by electric brush. The voltage of the SASTS is monitored by a voltage meter. When switch K1

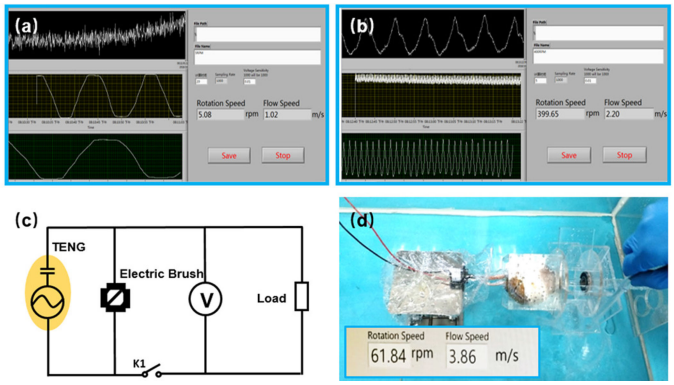

Fig. 5. Application demonstrations of the SASTS. (a–b) Real time test by the SASTS in different setting speeds. (c) Circuit diagram of the SASTS (a TENG, an electric brush and a voltmeter). (d) Demonstration of the SASTS system testing the real water speed.

is on, voltmeter start to process the data from the SASTS and export the rotation speed and the flow speed. Fig. 5(d) shows the photograph of the SASTS in testing water flow speed. When the SASTS was driven by water flow, it would rotate and the rotation speed of the sensor and the water flow speed of the water would be shown on the computer (Movie S3-S4).

III. Conclusion

We designed a fully enclosed self-powered active spherical triboelectric velocity sensor that works on the relationship between the working frequency of device and fluid speed. By optimizing the structure parameter, the larger inner sphere shows better performance and the precision of average standard deviation is less than 4. This sensor has a wide detection range (rotation speed from 0.5 rpm to 500 rpm, flowing speed from 2 m/s to 16 m/s). Also, it works by contacting electrification at the rolling interface, which dramatically decrease the mechanical wear of materials, which exhibits a long stability more than half a year. Furthermore, SASTS could constitute a self-power sensor system to develop reliable, independent, sustainable, and continuous operation of sensing networks.

IV. Experimental Methods

Fabrication of the sensor. Firstly, prepare two 100 nm copper films as two electrodes on the inner surface of the acrylic hollow sphere (dimeter = 7 cm) by magnetron sputtering (Discovery635). Secondly, prepare two copper wires and connected with two electrodes. Then, mix the part A and Part B of the silicone rubber (Exoflex 0050 manufactured by Smooth-On) according to volume ratio 1:1. Smeared the mixture of part A and Part B of the silicone rubber (Exoflex 0050 manufactured by Smooth-On) on the inner surface of an acrylic ball. The mixed material was cured after six hours. Then tear off the soft film carefully. At the end, inject some water into the hollow soft silicone ball by the syringe and sealed the hole with little mixed silicone rubber.

Methods for measuring performance of the sensor. The sensor was driven by a rotary motor (86HSZ8N) to simulate the environment. The outputs were tested by a precision electrical meter (Keithley 6514). An electric brush (MOFLON MW) was used to connect the rotary circuit.

References

[1] W. Gao *et al.*, "Fully integrated wearable sensor arrays for multiplexed in situ perspiration analysis," *Nature*, vol. 529, pp. 509–514, 2016.
[2] S. Wang, L. Lin, and Z. L. Wang, "Triboelectric nanogenerators as self-powered active sensors," *Nano Energy*, vol. 11, pp. 436–462, 2015.
[3] Z. L. Wang, "Triboelectric nanogenerators as new energy technology for self-powered systems and as active mechanical and chemical sensors," *ACS Nano*, vol. 7, no. 11, pp. 9533–9557, 2013.
[4] C. Giupponi, V. Mojtahed, A. K. Gain, C. Biscaro, and S. Balbi, "Chapter 6 - Integrated Risk Assessment of Water-Related Disasters," in *Hydro-Meteorological Hazards, Risks and Disasters*, J. F. Shroder, P. Paron, and G. D. Baldassarre, Eds. Boston: Elsevier, pp. 163–200, 2015.
[5] T. G. Veenema, C. P. Thornton, R. P. Lavin, A. K. Bender, S. Seal, and A. Corley, "Climate change–related water disasters' impact on population health," *J. Nurs. Scholarship*, vol. 49, no. 6, pp. 625–634, 2017.
[6] M. Kim and W. Moon, "A new linear encoder-like capacitive displacement sensor," *Measurement*, vol. 39, no. 6, pp. 481–489, 2006.
[7] A. H. Kadhim, T. K. M. Babu, and D. O. Kelly, "Measurement of steady-state and transient load-angle, angular velocity, and acceleration using an optical encoder," *IEEE Trans. Instrum Meas.*, vol. 41, no. 4, pp. 486–489, Aug. 1992.
[8] E. Zabler, F. Heintz, R. Dietz, and G. Gerlach, "Mechatronic sensors in integrated vehicle architecture," *Sens. Actuator. A Phys.*, vol. 31, no. 1, pp. 54–59, 1992.
[9] X. Xie *et al.*, "Impedance matching effect between a triboelectric nanogenerator and a piezoresistive pressure sensor induced self-powered weighing," *Adv. Mater. Technol.*, vol. 3, no. 6, 2018, Art. no. 1800054.
[10] Q. Shen *et al.*, "Self-powered vehicle emission testing system based on coupling of triboelectric and chemoresistive effects," *Adv. Funct. Mater.*, vol. 28, no. 10, 2018, Art. no. 1703420.
[11] X. J. Pu *et al.*, "Eye motion triggered self-powered mechnosensational communication system using triboelectric nanogenerator," *Sci. Adv.*, vol. 3, no. 7, 2017, Art. no. e1700694.
[12] Z. Wen *et al.*, "Self-powered textile for wearable electronics by hybridizing fiber-shaped nanogenerators, solar cells, and supercapacitors," *Sci. Adv.*, vol. 2, no. 10, 2016, Art. no. e1600097.
[13] L. Xie *et al.*, "Spiral steel wire based fiber-shaped stretchable and tailorable triboelectric nanogenerator for wearable power source and active gesture sensor," *Nano-micro. Lett.*, vol. 11, no. 1, p. 39, 2019.
[14] K. Yan *et al.*, "Phosphorus mitigation remains critical in water protection: A review and meta-analysis from one of China's most eutrophicated lakes," *Sci. Total Environ.*, vol. 689, pp. 1336–1347, 2019.
[15] H. Ouyang *et al.*, "Self-powered pulse sensor for antidiastole of cardiovascular disease," *Adv. Mater.*, vol. 29, no. 40, 2017, Art. no. 1703456.
[16] X. Zhang *et al.*, "Self-powered distributed water level sensors based on liquid–solid triboelectric nanogenerators for ship draft detecting," *Adv. Funct. Mater.*, vol. 29, no. 41, 2019, Art. no. 1900327.
[17] Y. Zou *et al.*, "A bionic stretchable nanogenerator for underwater sensing and energy harvesting," *Nat. Commun.*, vol. 10, 2019, Art. no. 2695.
[18] X. S. Meng, H. Y. Li, G. Zhu, and Z. L. Wang, "Fully enclosed bearing-structured self-powered rotation sensor based on electrification at rolling interfaces for multi-tasking motion measurement," *Nano Energy*, vol. 12, pp. 606–611, 2015.
[19] M. Liu *et al.*, "Large-area all-textile pressure sensors for monitoring human motion and physiological signals," *Adv. Mater.*, vol. 29, no. 41, 2017, Art. no. 1703700.
[20] Z. Lin *et al.*, "Triboelectric nanogenerator enabled body sensor network for self-powered human heart-rate monitoring," *ACS Nano*, vol. 11, no. 9, pp. 8830–8837, 2017.
[21] J. Wang *et al.*, "Sustainably powering wearable electronics solely by biomechanical energy," *Nat. Commun.*, vol. 7, 2016, Art. no. 12744.
[22] L. Chen, Q. Shi, Y. Sun, T. Nguyen, C. Lee, and S. Soh, "Controlling Surface Charge Generated by Contact Electrification: Strategies and Applications," *Adv Mater*, vol. 30, no. 47, 2018, Art. no. 1802405.
[23] Q. Shi, T. He, and C. Lee, "More than energy harvesting – Combining triboelectric nanogenerator and flexible electronics technology for enabling novel micro-/nano-systems," *Nano Energy*, vol. 57, pp. 851–871, 2019.
[24] F.-R. Fan, Z.-Q. Tian, and Z. Lin Wang, "Flexible triboelectric generator," *Nano Energy*, vol. 1, no. 2, pp. 328–334, 2012.

[25] Y. Zi, S. Niu, J. Wang, Z. Wen, W. Tang, and Z. L. Wang, "Standards and figure-of-merits for quantifying the performance of triboelectric nanogenerators," *Nat. Commun.*, vol. 6, 2015, Art. no. 8376.
[26] Z. Wen *et al.*, "Toward self-powered photodetection enabled by triboelectric nanogenerators," *J. Mater. Chem. C*, vol. 6, no. 44, pp. 11893–11902, 2018.
[27] L. Han *et al.*, "Self-driven photodetection based on impedance matching effect between a triboelectric nanogenerator and a MoS_2 nanosheets photodetector," *Nano Energy*, vol. 59, pp. 492–499, 2019.
[28] H. Guo *et al.*, "A highly sensitive, self-powered triboelectric auditory sensor for social robotics and hearing aids," *Sci. Robot.*, vol. 3, no. 20, 2018, Art. no. eaat2516.
[29] G. Cheng *et al.*, "Managing and maximizing the output power of a triboelectric nanogenerator by controlled tip–electrode air-discharging and application for UV sensing," *Nano Energy*, vol. 44, pp. 208–216, 2018.
[30] L. Xu *et al.*, "Coupled triboelectric nanogenerator networks for efficient water wave energy harvesting," *ACS Nano*, vol. 12, no. 2, pp. 1849–1858, 2018.
[31] X. Liang *et al.*, "Triboelectric nanogenerator networks integrated with power management module for water wave energy harvesting," *Adv. Funct. Mater.*, vol. 29, 2019, Art. no. 1807241.
[32] P. Cheng *et al.*, "Largely enhanced triboelectric nanogenerator for efficient harvesting of water wave energy by soft contacted structure," *Nano Energy*, vol. 57, pp. 432–439, 2019.
[33] S. Wang, Y. Xie, S. Niu, L. Lin, and Z. L. Wang, "Freestanding triboelectric-layer-based nanogenerators for harvesting energy from a moving object or human motion in contact and non-contact modes," *Adv. Mater.*, vol. 26, no. 18, pp. 2818–2824, 2014.
[34] Q. Shi, H. Wang, T. Wang, and C. Lee, "Self-powered liquid triboelectric microfluidic sensor for pressure sensing and finger motion monitoring applications," *Nano Energy*, vol. 30, pp. 450–459, 2016.
[35] T. Chen *et al.*, "Triboelectric self-powered wearable flexible patch as 3D motion control interface for robotic manipulator," *ACS Nano*, vol. 12, no. 11, pp. 11561–11571, 2018.
[36] R. Hinchet*et al.*, "Transcutaneous ultrasound energy harvesting using capacitive triboelectric technology," *Science*, vol. 365, no. 6452, pp. 491–494, 2019.
[37] S. Wang, Y. Xie, S. Niu, L. Lin, and Z. L. Wang, "Freestanding triboelectric-layer-based nanogenerators for harvesting energy from a moving object or human motion in contact and non-contact modes," *Adv. Mater.*, vol. 26, no. 18, pp. 2818–2824, 2014.

Ping Cheng received the B.S. degree in light chemical engineering from the School of Zhejiang Sci-Tech University, Hangzhou, China, in 2016. She is currently working toward the Ph.D. degree with the School of Institute of Functional Nano & Soft Materials, Soochow University, Suzhou, China. After B.Sc. degree, she entered Soochow University and the Beijing Institute of Nanoenergy and Nanosystems, Chinese Academy of Sciences, as a joint student. Her research interest mainly focuses on triboelectric nanogenerator for blue energy.

Mingchao Sun received the B.S. degree in optical information science and technology from Jilin University, Changchun, China, in 2005, and the Ph.D. degree in optical engineering from the Changchun Institute of Optics, fine mechanics and physics, Chinese Academy of Sciences, Changchun, in 2012. His main research interest includes precision sensor data (signal) processing.

Chunlei Zhang received the B.S. degree in material science and engineering from the Nanjing University of Aeronautics and Astronautics University, Nanjing, China, in 2016.He is currently working toward the Postgraduate degree with the Beijing Institute of Nanoenergy and Nanosystems, Chinese Academy of Sciences, Beijing, China. His current research interest is triboelectric nanogenerator based on energy storage and self-power system.

Hengyu Guo received the B.S. and Ph.D. degrees in applied physics from Chongqing University, Chongqing, China. He is currently a Postdoctoral Fellow with the Zhong Lin Wang' group, Georgia Institute of Technology. His current research interest is triboelectric nanogenerator based energy and sensor systems.

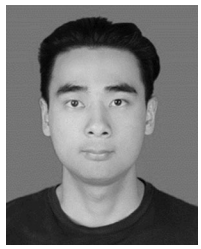

Jihong Shi received the B.S. degree in polymer materials science and engineering from the Qingdao University of Science and Technology, Qingdao, China, in 2017. He is currently a Graduate Student with the Institute of Functional Nano & Soft Materials, Soochow University. His main research interests focus on triboelectric nanogenerator based human–machine interface.

Yi Zhang received the B.S. degree in nano material and technology from the College of Nano Science and Technology, Soochow University, Suzhou, China, in 2018. She is currently a Graduate Student with the Institute of Functional Nano & Soft Materials, Soochow University, working under the guidance of Prof. X. Sun. Her current research interest is triboelectric nanogenerator and its application in self-powered sensor system.

Yina Liu received the B.S. degree in electrical and electronic engineering from Xi'an Jiaotong-Liverpool University, Suzhou, China, in 2011, and the Ph.D. degree in applied mathematics from the University of Liverpool, Liverpool, U.K., in 2015. She joined the Department of Mathematical Sciences, Xi'an Jiaotong-Liverpool University, as a Lecturer in January 2016. Her main research interests focus on modeling and optimization of industrial problems.

Jie Wang received the Ph.D. degree from Xi'an Jiaotong University, Xi'an, China, in 2008. He is currently a Professor with the Beijing Institute of Nanoenergy and Nanosystems, Chinese Academy of Sciences, Beijing, China. His current research interests focus on the energy materials, supercapacitors, nanogenerators, and self-powered systems.

Zhen Wen received the B.S. degree in materials science and engineering from the China University of Mining and Technology, Xuzhou, China, in 2011, and the Ph.D. degree in materials physics and chemistry from Zhejiang University, Hangzhou, China, in 2016. He is currently an Associate Professor with the Institute of Functional Nano & Soft Materials, Soochow University, Suzhou, China. During 2014–2016, he was supported by the program of China Scholarship Council as a Joint Ph.D. Student with the Georgia Institute of Technology. His main research interests focus on triboelectric nanogenerator for energy harvesting and self-powered sensing.

Xuhui Sun (Senior Member, IEEE) received the Ph.D. degree from the City University of Hong Kong, Hong Kong, in 2002. He performed postdoctoral research with the University of Western Ontario, Canada, from 2003 to 2005, and with NASA Ames Research Center, USA, from 2005 to 2007. He is currently a Full Professor with the Institute of Functional Nano & Soft Materials, Soochow University, Suzhou, China. He became a Research Scientist with NASA and an Adjunct Assistant Professor with Santa Clara University in 2007. His research interests include nanoelectronics, energy harvesting, nanosensors, and the development and application of synchrotron radiation techniques.